Physical Properties
of Carbon Nanotubes

Ao Teng

Course: Solid State II
Instructor: Elbio Dagotto
Spring 2010
Department of Physics
University of Tennessee
Email: ateng1@utk.edu

Physical Properties
of Carbon Nanotubes

Abstract:
Carbon nanotubes, as the prototypes of artificial one dimensional nano materials, have been intensely investigated since 1991. They originated from graphite sheets, but come along with some new physical properties due to quantum confinement. Soon after they were discovered, researchers realized their broad applications in prospect. In this paper, a brief introduction focusing on basic concepts and geometry of carbon nanotubes will be conducted, followed by a series of discussions on related electronic properties of carbon nanotubes, as well as other physical properties.

Contents:

I. Introduction

Physics down to the scale of nanometers has been a fascinating field for quite a long time, even back to more than 50 years ago, Richard Feynman realized that "There's Plenty of Room at the Bottom"[1] and predicted that nano science would be a new frontier. Multiwalled carbon nanotubes (MWNT), as hollow cylinders with diameters in the nanometer range,

consisting of carbon atoms, were first observed in 1991 by Sumio Iijima at the NEC Research Laboratory, when he studied the soot made from by-products obtained during the synthesis of fullerenes by the electric arc discharge method. [2] Two years later, single-wall carbon nanotubes (SWNT) were synthesized. [3][4]

II. Typical Synthesis Methods of Carbon Nanotubes

Generally, synthesis methods of carbon nanotubes can be classified into two main categories corresponding to different temperatures: The high temperature routes, such as the electric-arc discharge technique; the medium temperature routes (the most popular one is chemical vapor deposition).

A. Electric-Arc Discharge Technique

An electric-arc discharge is an electrical breakdown of a gas which produces an ongoing plasma, resulting from a current flowing through normally nonconductive media. In Iijima's initial experiment [2], he used a DC arc discharge in argon consisting of a set of carbon electrodes running at 2000-3000°C at nominal conditions of 100A and 20V. The modified version of this method could bring the temperature up to 6000°C and make the graphite to sublimate. As a consequence, carbon atoms are ejected from the solid and form plasma. These atoms will accumulate on the cathode, which is relatively colder. If small amounts of transition metals are introduced in the target graphite, the single-walled carbon nanotubes are the dominant product, otherwise formation of multiwalled carbon nanotubes will take place.

Fig. 1.
Left: Plasma from the electric-arc experiment performed by Thomas Ebbesen et al. [5]
Middle: 2 sheets carbon nanotube, adapted from Iijima's paper [2].
Right: By printing patterns of catalyst particles on the substrate, Hongjie Dai et al. have been able to control where the tubes form with chemical vapor deposition method. [5]

B. Chemical Vapor Deposition

With transition-metal particles as growth germs, the carbon containing gaseous compounds at temperature 600-1100˚C will decompose on those sites and form carbon filaments of various sizes and shapes including nanotubes. Typical compounds are carbon monoxide or hydrocarbons.

III. Structure and Symmetry of Carbon Nanotubes

The topological structure of SWNT is quite like modified single sheet graphene, thus the tubes are usually labeled in terms of the graphene lattice vectors.
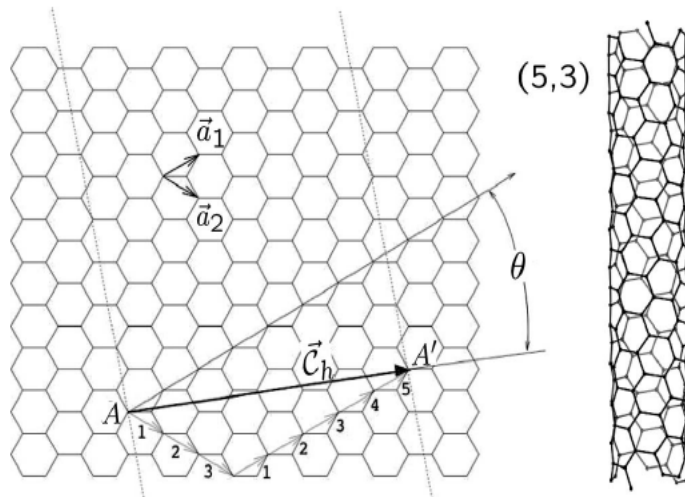
Fig. 2. Graphene lattice vectors a_1 and a_2. The chiral vector $Ch=5a_1+3a_2$ represents a possible wrapping of the two-dimensional graphene sheet into a tubular form. The direction perpendicular to Ch is the tube axis. The chiral angle θ is defined by the Ch vector and the a_1 zigzag direction of the graphene lattice. In the present example, a (5, 3) nanotube is under construction and the resulting tube is illustrated below. [6]
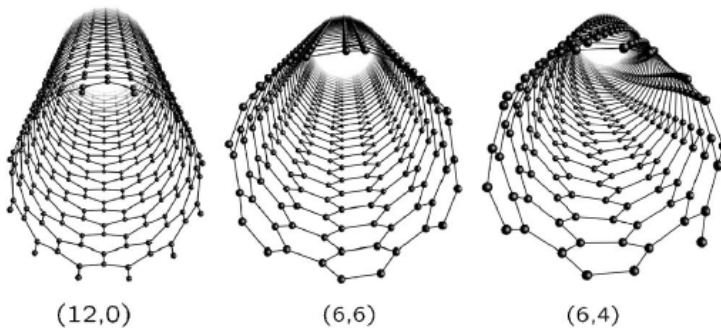
Fig.3. Atomic structures of
(12, 0) zigzag,
(6, 6) armchair, and
(6, 4) chiral nanotubes.

TABLE I. Structural parameters for a (n, m) carbon nanotube. n, m, t1, t2 are integers. [6]

Symbol	Name	Formula	Value
a	lattice constant	$a=\sqrt{3}a_{cc}\approx 2.46$ Å	$a_{cc}\approx 1.42$ Å
$\mathbf{a_1, a_2}$	basis vectors	$\left(\dfrac{\sqrt{3}}{2};\dfrac{1}{2}\right)a, \left(\dfrac{\sqrt{3}}{2};-\dfrac{1}{2}\right)a$	
$\mathbf{b_1, b_2}$	reciprocal-lattice vectors	$\left(\dfrac{1}{\sqrt{3}};1\right)\dfrac{2\pi}{a}, \left(\dfrac{1}{\sqrt{3}};-1\right)\dfrac{2\pi}{a}$	
$\mathbf{C}_h$	chiral vector	$\mathbf{C}_h=n\mathbf{a_1}+m\mathbf{a_2}\equiv(n,m)$	$(0\leq|m|\leq n)$
d_t	tube diameter	$d_t=\dfrac{|\mathbf{C}_h|}{\pi}=\dfrac{a}{\pi}\sqrt{n^2+nm+m^2}$	
θ	chiral angle	$\sin\theta=\dfrac{\sqrt{3}m}{2\sqrt{n^2+nm+m^2}}$	$0\leq|\theta|\leq\dfrac{\pi}{6}$
		$\cos\theta=\dfrac{2n+m}{2\sqrt{n^2+nm+m^2}}$	$\tan\theta=\dfrac{\sqrt{3}m}{2n+m}$
$\mathbf{T}$	translational vector	$\mathbf{T}=t_1\mathbf{a_1}+t_2\mathbf{a_2}\equiv(t_1,t_2)$	$\gcd(t_1,t_2)=1^{\text{a}}$
		$t_1=\dfrac{2m+n}{N_R}, t_2=-\dfrac{2n+m}{N_R}$	$N_R=\gcd(2m+n,2n+m)^{\text{a}}$
N_C	number of C atoms per unit cell	$N_C=\dfrac{4(n^2+nm+m^2)}{N_R}$	

[a] $\gcd(n,m)$ denotes the greatest common divisor of the two integers n and m.

The symmetry of carbon nanotubes is described by line groups, which are the full space groups of one-dimensional systems including point-group symmetries (e.g. rotations or reflections) and translations. Damnjanović et al. showed that every nanotube with a particular chirality (n,m) belongs to a different line group. [7][8] Only armchair and zig-zag tubes with the same n belong to the same symmetry group.
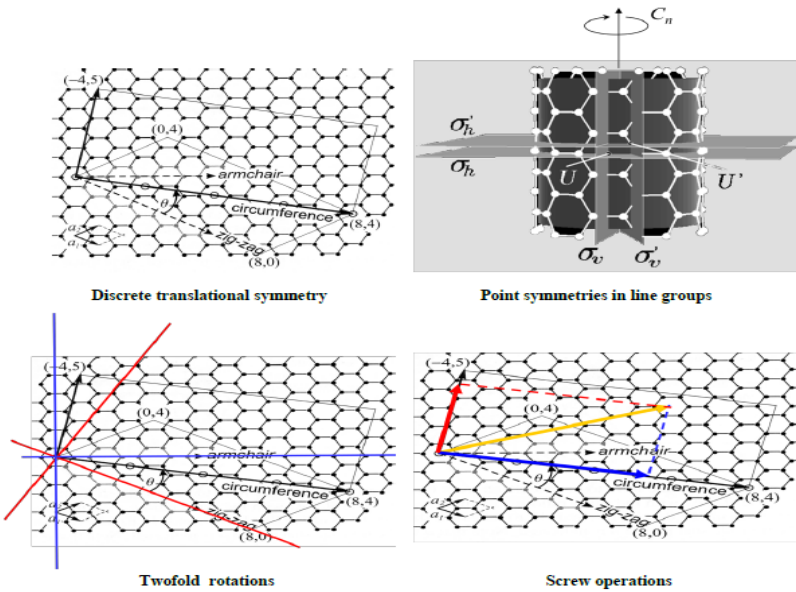
Fig.4. Symmetries in SWNT

IV. Electronic Properties of Carbon Nanotubes

Carbon nanotubes have two types of bonds due to sp^2 hybridization: the σ bonds, which are along the cylinder wall and form the hexagonal network; and the π bonds which interact between different tubes (Van-der Waals Force). Unexpectedly, the in-plane σ bonds don't play an important role in the electronic properties (e.g., electronic transport or optical absorption in the visible energy range) of carbon nanotubes because they are far away from Fermi level. In contrast, the bonding and antibonding π bands cross the Fermi level. [9] See **Fig.5.**
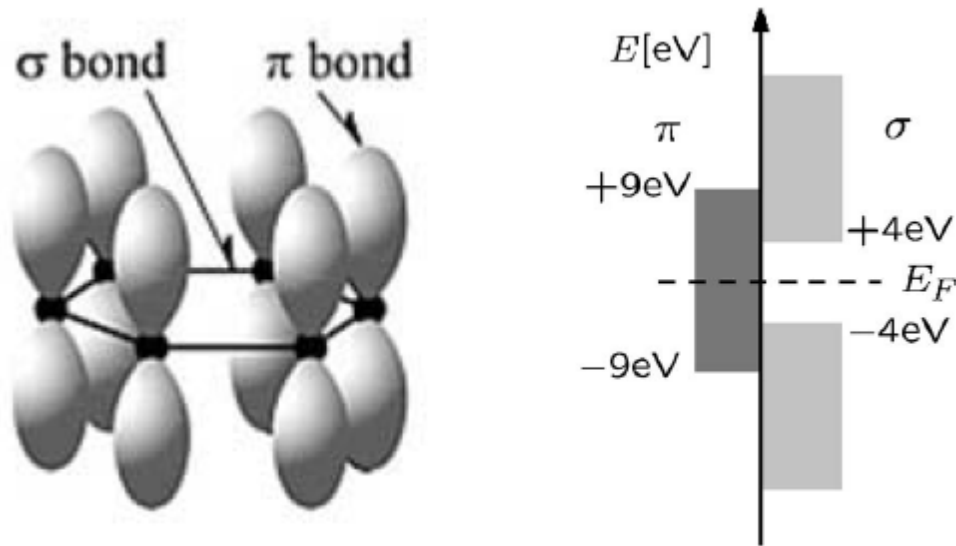
Fig.5. Scheme of sp^2 hybridization in graphene; σ bonds, π bonds and their energies with respect to Fermi level. Adapted from [10].

A. Reciprocal space and Brillouin zone
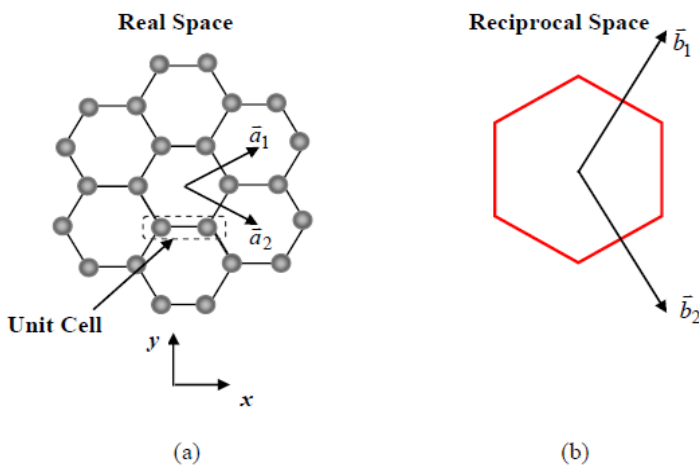
Fig.6. Refer to Table I,
$$a = \sqrt{3}a_{cc} = 2.46\text{Å}$$
$$\mathbf{a}_1 = a\left(\frac{\sqrt{3}}{2}\hat{\mathbf{x}} + \frac{1}{2}\hat{\mathbf{y}}\right)$$
$$\mathbf{a}_2 = a\left(\frac{\sqrt{3}}{2}\hat{\mathbf{x}} - \frac{1}{2}\hat{\mathbf{y}}\right)$$
$$\mathbf{b}_1 = \frac{2\pi}{a}\left(\frac{1}{\sqrt{3}}\hat{\mathbf{x}} + 1\hat{\mathbf{y}}\right)$$
$$\mathbf{b}_2 = \frac{2\pi}{a}\left(\frac{1}{\sqrt{3}}\hat{\mathbf{x}} - 1\hat{\mathbf{y}}\right)$$

The enclosed hexagonal region in (b) is Brillouin zone.

B. Tight-binding model and band structure

In analogy with graphene, for given carbon atom, there are three nearest neighbors, as highlighted in **Fig.7.** For a single, flat graphene sheet, symmetry forbids coupling of π bands to σ bands that are well below and well above the Fermi energy. The π bands are well represented as linear combinations of p_z orbitals of the carbon atoms, where z is perpendicular to the plane. Two bands of p_z states will emerge due to the fact that graphene has two atoms per cell.
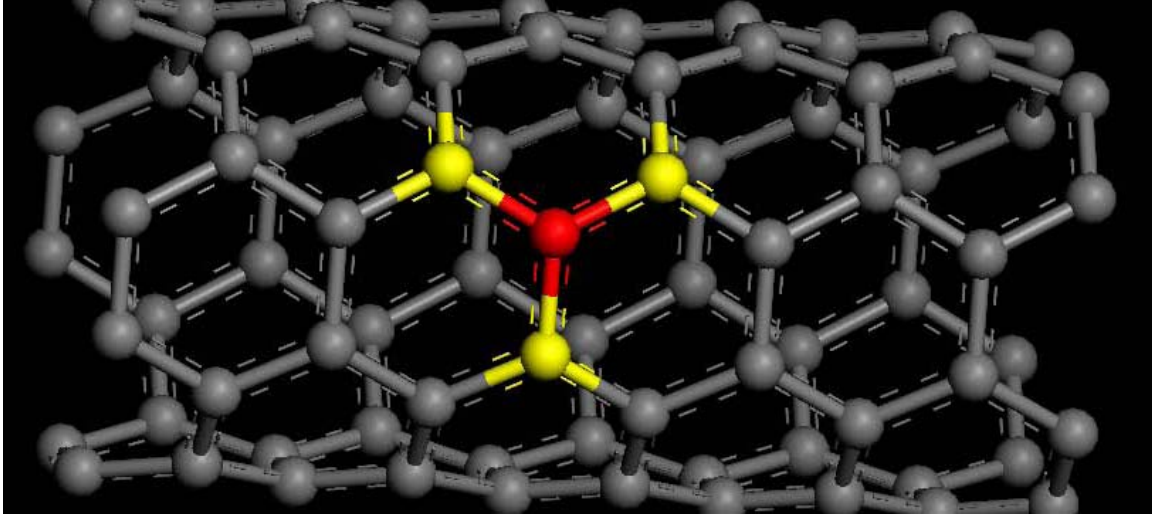
Fig.7. Consider area near the red ball as two-dimensional plane. If we define the coordinates of the red ball as (0, 0), then the three nearest neighbors are $(0, -\frac{a}{\sqrt{3}})$, $(-\frac{a}{2}, \frac{a}{2\sqrt{3}})$, $(\frac{a}{2}, \frac{a}{2\sqrt{3}})$, respectively.

Continue with the assumption of linear combination of atomic orbitals (LCAO), we could follow Kittel's textbook [11] and write:

$$\psi_k(\mathbf{r}) = \sum_j C_{kj}\, \varphi(\mathbf{r} - \mathbf{r_j}) \tag{1}$$

In which $\varphi(\mathbf{r})$ is the wave function for free electron moving in the electric field of isolated atom. To construct Bloch functions, let $C_{kj} = \dfrac{e^{i\mathbf{k}\cdot\mathbf{r_j}}}{\sqrt{N}}$, N is normalized number (number of atoms in the system). Thus,

$$\psi_k(\mathbf{r}) = N^{-1/2} \sum_j e^{(i\mathbf{k}\cdot\mathbf{r_j})}\varphi(\mathbf{r}-\mathbf{r_j}) \tag{2}$$

To calculate modified energy,

$$\langle \mathbf{k}|H|\mathbf{k}\rangle = N^{-1}\sum_{j,m} e^{i\mathbf{k}\cdot(\mathbf{r_j}-\mathbf{r_m})}\left\langle \varphi_m\left|H\right|\varphi_j\right\rangle \tag{3}$$

In which $\varphi_m = \varphi(\mathbf{r}-\mathbf{r_m})$

Let $\boldsymbol{\rho_m} = \mathbf{r_m} - \mathbf{r_j}$

$$\langle \mathbf{k}|H|\mathbf{k}\rangle = \sum_m e^{(-i\mathbf{k}\cdot\boldsymbol{\rho_m})}\int dV\varphi^*(\mathbf{r}-\boldsymbol{\rho_m})\,H\varphi(\mathbf{r}) \tag{4}$$

$$= \gamma_0 \sum_m e^{(-i\mathbf{k}\cdot\boldsymbol{\rho_m})}, \qquad \text{in the case } \left\langle \mathbf{k}\left|H^{(0)}\right|\mathbf{k}\right\rangle = 0,$$

$$\gamma_0 = \int dV\varphi^*(\mathbf{r}-\boldsymbol{\rho_m})\,H\varphi(\mathbf{r}) \quad \text{for nearest neighbor}$$

Plug $(0, -\frac{a}{\sqrt{3}})$, $(-\frac{a}{2}, \frac{a}{2\sqrt{3}})$, $(\frac{a}{2}, \frac{a}{2\sqrt{3}})$ into the expression yields

$$H_{12}(\mathbf{k}) = \gamma_0[e^{\frac{ik_y a}{\sqrt{3}}} + e^{\frac{ik_x a}{2}-\frac{ik_y a}{2\sqrt{3}}} + e^{-\frac{ik_x a}{2}-\frac{ik_y a}{2\sqrt{3}}}], \tag{5}$$

$H_{12}(\mathbf{k})$ is specified in the in-secular equation

$$\left|\hat{H}(\mathbf{k}) - \varepsilon(\mathbf{k})\right| = \begin{vmatrix} -\varepsilon(\mathbf{k}) & H_{12}(\mathbf{k}) \\ H_{12}^*(\mathbf{k}) & -\varepsilon(\mathbf{k}) \end{vmatrix} = 0$$

Eventually we get

$$\varepsilon(\mathbf{k}) = \pm|H_{12}(\mathbf{k})| = \pm\gamma_0[1 + 4\cos\left(k_y\frac{\sqrt{3}a}{2}\right)\cos(k_x\frac{a}{2}) + 4\cos^2((k_x\frac{a}{2})]^{1/2}$$

$$\tag{6}$$
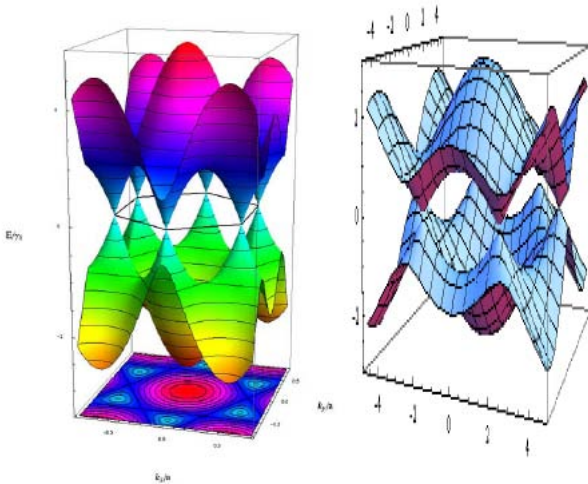
Fig.8

Left: Band structure and first Brillouin zone from wikipedia.

Right: Reproduced with Mathematica, γ_0 and a in arbitrary units.

C. Zone-folding approximation and metallicity

From the symmetry (and periodic boundary conditions) we know that the allowed wave vectors "around" the nanotube circumference are quantized, namely,

$$\psi_k(\mathbf{r} + \mathbf{C_h}) = e^{i\mathbf{k}\cdot\mathbf{C_h}}\psi_k(\mathbf{r}) \tag{7}$$

$$\mathbf{C_h} = n\mathbf{a_1} + m\mathbf{a_2}$$

$$\mathbf{k} = n'\mathbf{b_1} + m'\mathbf{b_2}$$

$$\mathbf{k}\cdot\mathbf{C_h} = 2\pi(nn' + mm') = 2\pi l, \qquad l \text{ is integer} \tag{8}$$

Along the nanotube axis, in contrast, the wave vectors are continuous. If we plot those allowed wave vectors onto the Brillouin zone of graphene, we will find a series of parallel lines defined by **Eq. (8)**, See **Fig.9.** The idea of the zone-folding approximation is that the electronic band structure of a specific nanotube is given by superposition of the graphene electronic energy bands along the corresponding allowed k lines.
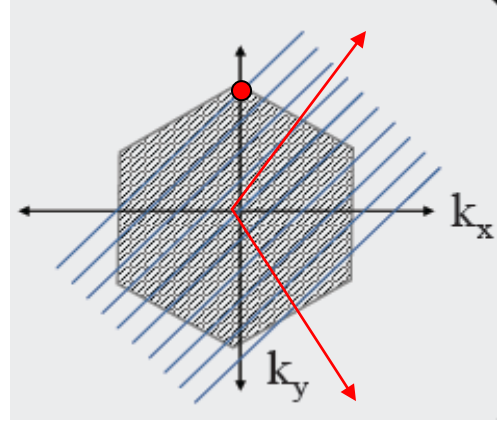
Fig.9. Allowed k lines. [12]

Metal is known for having filled states around Fermi level. In another word, to be "metallic", the graphene K point is supposed to be among the allowed states. Otherwise the nanotube is semiconducting with a moderate band gap. For instance, take the highlighted point in **Fig.9**,

$$\mathbf{k} = \frac{1}{3}\mathbf{b_1} - \frac{1}{3}\mathbf{b_2} \qquad\qquad (n' = \frac{1}{3}, m' = -\frac{1}{3})$$

Plugging into **Eq. (8)** yields $(n - m) = 3l$ \hfill (9)

The condition (n−m) =3l is always satisfied for armchair tubes and for the subset of the (n, 0) zigzag tubes with n multiples of 3.

D. Density of states (DOS) and Van Hove singularities

The density of states $\frac{\Delta N}{\Delta E}$ represents the number of available states for given energy interval. In this paragraph, theoretical calculation has been avoided, only experimental measurement and related physical concepts are sketched. The shape of the DOS depends on dimensionality, as shown below. These "spikes" in the DOS of 1D system are called Van Hove singularities and originate from the confinement properties in directions perpendicular to the tube axis.
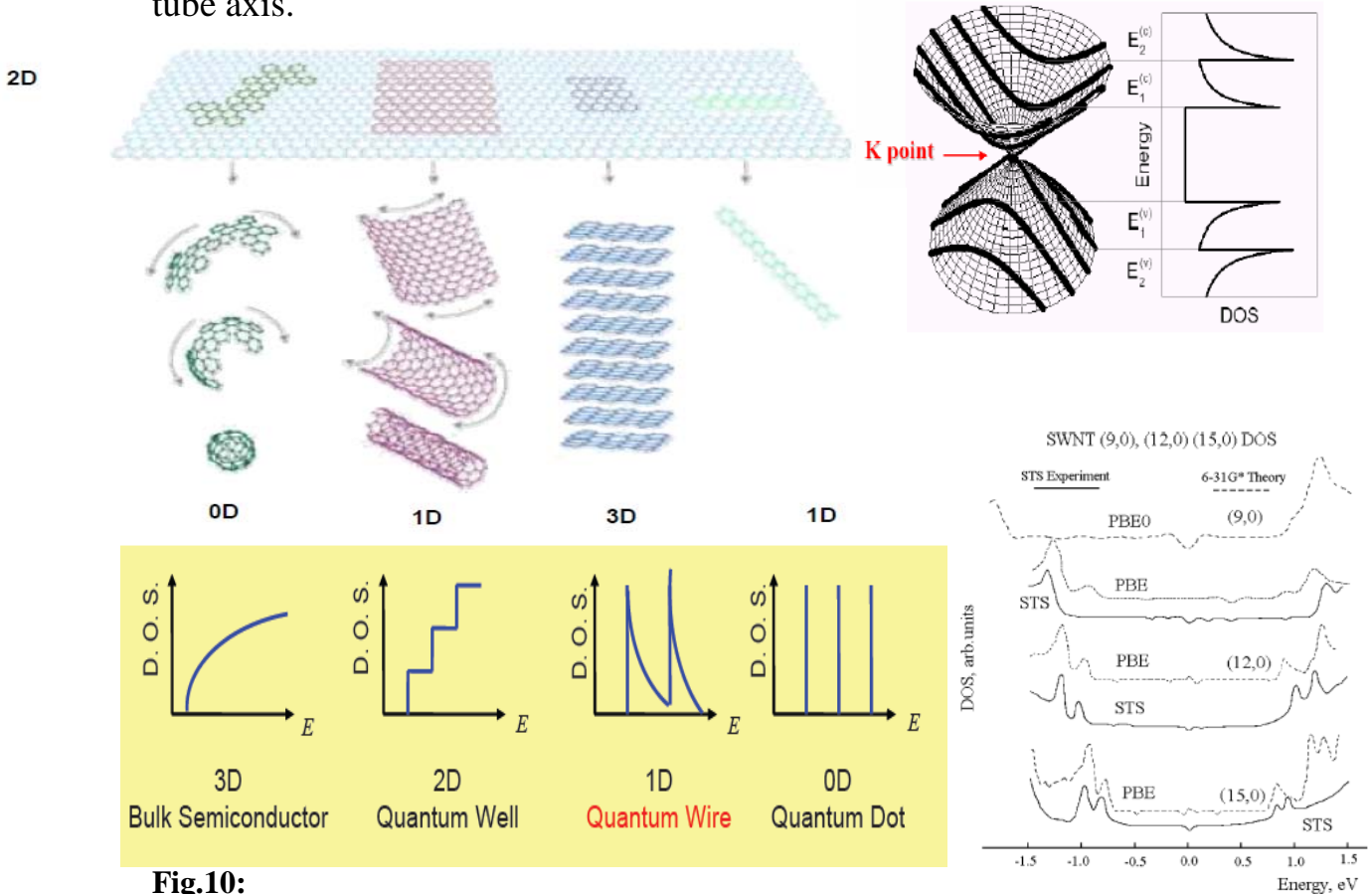
Fig.10:

Left Top: Classifications of Carbon nanomaterials

Left Bottom: DOS for different dimensionalities [13]

Right Top: Van Hove singularities due to confinement of 1D electronic state on cutting lines [13]

Right Bottom: Experimental spectra (solid line) compared with calculated data (dashed line). [14]

With Scanning Tunneling Spectroscopy (STS), people could really measure DOS. [15]

$$\left(\frac{dI}{dU}\right)_{U=V} \approx \rho_{sample}\ (E_F + eV)\rho_{Tip}\ (E_F) \tag{10}$$

It's interesting to notice those "spikes" in the DOS of 1D nanomaterial caused by the so called "Van Hove singularities". Consider the energy and eigenstate of an ideal nanotube which is confined along x and y axes (~nm) but infinite along z axis:

$$\varepsilon = \varepsilon_{i,j} + \frac{\hbar^2 k_z^2}{2m}; \qquad \psi(x, y, z) = \psi_{i,j}(x, y)e^{ikz} \tag{11}$$

In analogy with a rectangle, the solution for $\varepsilon_{i,j}$ and $\psi_{i,j}(x, y)$ are similar to the 2D"particle in a box" problem. [11]

$$D(\varepsilon) = \sum_{i,j} D_{i,j}(\varepsilon)$$

$$D_{i,j}(\varepsilon) = \sum_{i,j} \frac{dN_{i,j}}{dk}\frac{dk}{d\varepsilon} = \sum_{i,j} 2 \cdot 2 \cdot \frac{L}{2\pi}\left[\frac{m}{2\hbar^2(\varepsilon-\varepsilon_{i,j})}\right]^{1/2} = \begin{cases} \frac{4L}{h\nu_{i,j}}, & \varepsilon > \varepsilon_{i,j} \\ 0, & \varepsilon < \varepsilon_{i,j} \end{cases} \tag{12}$$

The first "2" comes from spin degeneracy; the second"2" is due to k has both positive and negative values; $v_{i,j}$ is the velocity of electron with kinetic energy$(\varepsilon - \varepsilon_{i,j})$. Near the "watershed" at $\varepsilon_{i,j}$, DOS will disperse due to the term$(\varepsilon - \varepsilon_{i,j})^{-1/2}$, this trait is called "Van Hove singularities".

V. Other Physical Properties

Compared with other materials, carbon nanotubes have a series of extraordinary properties. (Fig 11) First of all, their sizes are small enough to be used in microscopic research. For instance, nanotube is already used to replace traditional tungsten tip because its shape is relatively stable. Second, its tensile strength extremely larger than high-strength steel alloys (45 billion pascals versus ~2 billion pascals). Third, its current carrying capacity is estimated to be 1billion amps per square centimeter (copper wires burn out at about 1 million amps per square centimeter). Besides, its heat transmission efficiency and temperature stability are both appreciably larger than traditional materials.
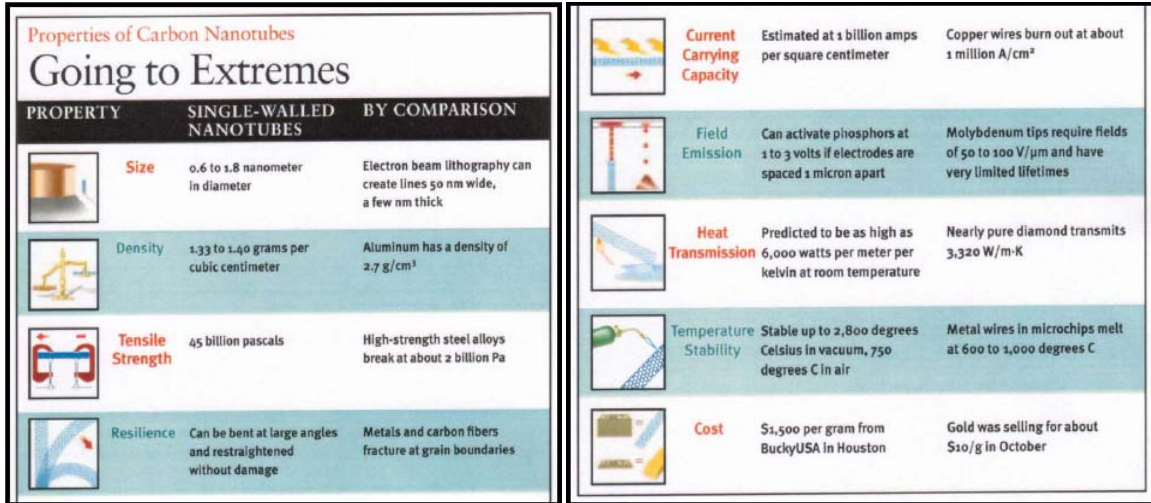
Fig.11. Other properties of Carbon nanotubes [5]

References:

[1]"There's Plenty of Room at the Bottom" is the topic of a classic talk that Richard Feynman gave on December 29th 1959 at the annual meeting of the American Physical Society at the California Institute of Technology.

The transcript of the talk is available online:
http://www.zyvex.com/nanotech/feynman.html

[2] Iijima, S., 1991, Nature (London) 354, 56.

[3] Iijima, S., and T. Ichihashi, 1993, Nature (London) 363, 603.

[4] Bethune, D. S., C. H. Kiang, M. S. de Vries, G. Gorman, R.Savoy, J.Vazquez, and R. Beyers, 1993, Nature (London) 363, 605.

[5] P. G. Collins and Ph. Avouris, Scientific American, 283, 62 (2000)

[6] Jean-Christophe Charlier, Blase, and Roche: Electronic and transport properties of nanotubes, Rev. Mod. Phys., Vol. 79, No. 2, April–June (2007)

[7] M.Damnjanović et al., "Full symmetry, optical activity, and potentials of single-wall and multiwall nanotubes", Phys.Rev.B 60, 2728 (1999)

[8] Reich, S., C. Thomsen, and J. Maultzsch, 2004, Carbon Nanotubes, Basic Concepts and Physical Properties (Wiley-VCH Verlag GmbH, Weinheim).

[9] Charlier, J.-C., X. Gonze, and J.-P. Michenaud, 1991, Phys.Rev. B 43, 4579.

[10] Loiseau, A., P. Launois, P. Petit, S. Roche, and J.-P. Salvetat, 2006, Understanding Carbon Nanotubes From Basics to Applications, Lecture Notes in Physics Vol. 677 (Springer-Verlag, Berlin).

[11]Charles Kittel, 2005, Introduction to Solid State Physics, 8th ed. (John Wiley & Sons, New York)

[12] Mintmire, J. W., and C. T. White, 1998, Phys. Rev. Lett. 81, 2506.

[13]Gene Dresselhaus, 2008, The Novel Nanostructures of Carbon (Condensed Matter Symposium, Purdue University)

[14] Pavel V. Avramov ,1, Konstantin N. Kudin, Gustavo E. Scuseria, 2003, Chemical Physics Letters 370, 597

[15] Julian Chen, 2008, Introduction to Scanning Tunneling Microscopy (Oxford Science Publication)